Available online at www.sciencedirect.com

SCIENCE DIRECT®

Journal of Mathematical Psychology 50 (2006) 411–420

Journal of Mathematical Psychology

www.elsevier.com/locate/jmp

Analysis of a two-alternative force-choice signal detection theory model

Mikhail Katkov, Misha Tsodyks, Dov Sagi*

Department of Neurobiology/Brain Research, The Weizmann Institute of Science, Rehovot 76100, Israel

Received 19 October 2004; received in revised form 3 October 2005
Available online 30 January 2006

Abstract

A basic problem in psychophysics is recovering the mean internal response and noise amplitude from sensory discrimination data. Since these components cannot be estimated independently, several indirect methods were suggested to resolve this issue. Here we analyze the two-alternative force-choice method (2AFC), using a signal detection theory approach, and show analytically that the 2AFC data are not always suitable for a reliable estimation of the mean internal responses and noise amplitudes. Specifically, we show that there is a subspace of internal parameters that are highly sensitive to sampling errors (singularities), which results in a large range of estimated parameters with a finite number of experimental trials. Four types of singular models were identified, including the models where the noise amplitude is independent of the stimulus intensity, a situation often encountered in visual contrast discrimination. Finally, we consider two ways to avoid singularities: (1) inserting external noise to the stimuli, and (2) using one-interval forced-choice scaling methods (such as the Thurstonian scaling method for successive intervals).

Keywords: Psychophysics; 2AFC; Signal detection theory; Signal; Noise; Thurstonian scaling; SDT

1. Introduction

Human performance in psychophysical tasks, where stimuli with different intensities have to be discriminated, depends on the magnitude of internal responses within the brain, and on their trial-by-trial variability (Green & Swets, 1966; Thurstone, 1927). Knowledge of these response parameters is important for understanding the characteristics of the internal modules that process the presented stimuli. Unfortunately, these parameters cannot be measured independently with psychophysical tools. Recent attempts to resolve this issue in the case of contrast discrimination led to conflicting results with internal noise magnitude either increasing with contrast (Kontsevich, Chen, & Tyler, 2002; Lu & Dosher, 1999) or being constant (Gorea & Sagi, 2001), or approximately constant (Foley & Legge, 1981). In this work, we analyze a model derived from signal detection theory (SDT) for the two-alternative force-choice experimental method (2AFC) and show its theoretical limits in separating signal from internal noise (trial-by-trial variability of the signal). In an accompanying paper (Katkov, Tsodyks, & Sagi, 2006a) we apply the results of this theoretical analysis to measurements made with the contrast discrimination task.

In the 2AFC procedure an observer reports which one of two stimuli presented in a trial contains a target, with the target presented in only one of the two stimuli (e.g., the target is the stimulus with the higher intensity). SDT assumes that each stimulus evokes a scalar internal response that varies across trials so that the observer's performance depends on the distributions of these internal responses. In practice two simplifying assumptions are usually added: (1) the distribution of internal responses is normal, and (2) the decision is made by comparing internal responses corresponding to the two stimuli. Under these assumptions the 2AFC-SDT model is equivalent to the Thurstonian law of comparative judgment (Thurstone, 1927). The percentage of correct discrimination responses in these models is given by Green and Swets (1966), Iverson (1987)

*Corresponding author. Fax: +972 8934 4131.
E-mail address: Dov.Sagi@Weizmann.ac.il (D. Sagi).

0022-2496/$ - see front matter © 2005 Elsevier Inc. All rights reserved.
doi:10.1016/j.jmp.2005.11.002

and Thurstone (1927)

$$P_{s_1,s_2} = \Phi\left(\frac{R_{s_2} - R_{s_1}}{\sqrt{\sigma_{s_1}^2 + \sigma_{s_2}^2}}\right), \qquad (1)$$

where $\Phi(x)$ is a normal cumulative distribution function, R_{s_1}, R_{s_2} are mean internal responses, σ_{s_1}, σ_{s_2} are trial-by-trial standard deviations of the internal responses, and P_{s_1,s_2} is the probability of correct discrimination between stimuli s_1 and s_2. The values of P_{s_1,s_2} are estimated from the experiment, whereas those of R and σ are the parameters of the model. Eq. (1) has four unknown variables for one pair of stimulus intensities, leading to an ambiguous solution for the values of R and σ.

It seems to be possible to estimate the values of R and σ for all stimuli by increasing the number of stimuli with different intensities and the number of pairs for comparison, since the number of independent parameters grows linearly with the number of stimuli, whereas the number of pairs is a quadratic function of the number of stimuli. The problem was first formulated by Thurstone in his theory of comparative judgment (Thurstone, 1927), in which he described a practical procedure to obtain the unknown parameters in the case of a weak dependency of the σ's on the stimulus, where the problem can be linearized (Thurstone, 1927; Torgerson, 1958). Nevertheless, to solve the problem two conditions should be satisfied: (1) the set of equations (1) has a unique solution or a reasonable normalization is provided to remove ambiguity; (2) when an exact solution is unique a reliable estimation of the parameters from a limited number of trials can be obtained.

The first condition was analyzed in the work of Iverson (1987). He found that there are two types of symmetries in the models described by Eq. (1). (1) for any $\alpha > 0$, and β the following family of models:

$$R_i' = \alpha R_i + \beta,$$
$$\sigma_i' = \alpha \sigma_i \qquad (2)$$

describes exactly the same $P_{i,j}$ (continuous symmetry). (2) If there is a linear relationship between R and σ, then another model (with appropriately chosen constants a, b, c, d and k)

$$R_i' = \frac{aR_i + b}{cR_i + d} \quad \text{and} \quad \sigma_i' = \frac{k}{\sigma_i} \qquad (3)$$

describes exactly the same $P_{i,j}$ (point symmetry). Thus, even for infinitely long experiments the reconstruction of model parameters is only possible up to a common scaling factor for all parameters and for some constant added to all R's, because these transformations do not change the performances predicted by Eq. (1). In addition, when R and σ are linearly related, another solution will describe $P_{i,j}(R, \sigma)$.

It is possible to generalize the Thurstonian method by using any of the standard estimators. In practice, even for exactly specified and known internal parameters (R, σ), the measured performances deviate from the ones calculated by Eq. (1) owing to finite sampling. Thus, the model's parameters, estimated from the measured performances, deviate from the "true" parameters characterizing the internal response. The degree of this deviation depends on the method used for estimating the parameters and on the number of trials for each measurement.

The second condition for the reliable parameter estimation depends on the properties of the estimator and the model itself. To illustrate the effects of these two factors we can examine the problem in the "P" space (Fig. 1), where coordinates are defined by the values of P_{s_1,s_2}, and each pair (s_1, s_2) represents an axis in multidimensional space. The dimensionality of the space is defined by the number of pairs selected for comparisons in the experiment. Eq. (1) defines the surface in this space, parameterized by the variables R's and σ's. This surface contains P-values that result from the SDT model described above for all possible parameter values R's and σ's. The experimentally measured values of P define a point in this space that does not lie on the surface, because of the finite sampling. The number of trials defines the size of the region in P space where possible measurements can be found (more precisely, for each point in the region, it defines its probability of being obtained in the experiment, given a true model). The estimator projects the measured point into the surface and finds the parameters corresponding to the projected point. Thus,

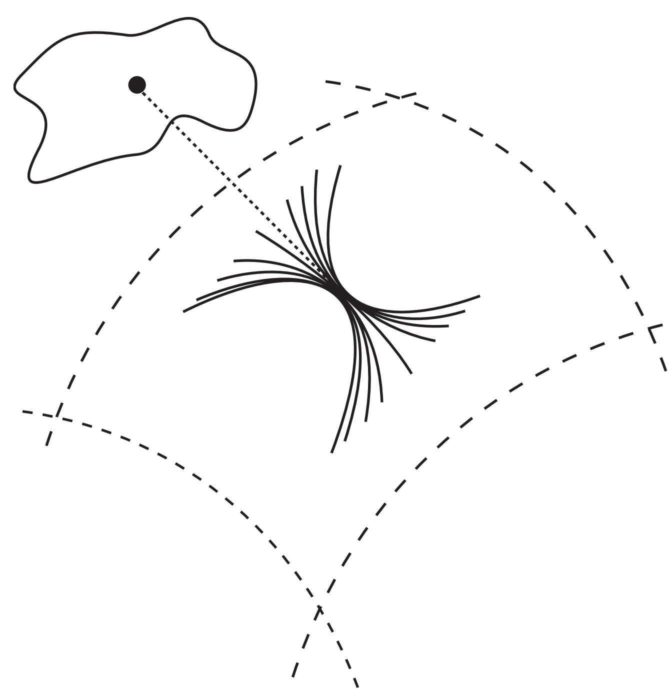

Fig. 1. An illustration of parameterization singularity. After the projection of measured performances onto the surface is performed by the estimator, the projected points can fall near the singular point of the parameterization where different values of the parameters correspond to very close points on the surface. Consequently, any estimator will not be able to distinguish between these parameters.

the shape and the size of the projected region (and possible parameters of the model) is defined by the estimator. If the parameterization of the surface by the R's and σ's has a singularity, then near the singular point, large changes in the parameters consequently lead to very small changes in the performances, which is reflected as a small shift on the surface. In this case a small experimental error will lead to large differences in the estimated parameters, independently of the estimator used. This, in turn, leads to large confidence intervals in the estimated parameters. We emphasize that ambiguity in parameter estimation resulting from singularity is different from the symmetry considerations described above.

The present work deals with the singularities in the parameterization of the model performances on the surface. The properties of particular estimators are not discussed here since singularities lead to difficulties in the estimation of the model parameters, regardless of the estimator used. The symmetries of the exact solution of Eq. (1) are described in Iverson (1987) and are not discussed here. The main issue here is the ability to estimate parameters of the model described by Eq. (1) from the experimental data, where limited number of trials lead to P_{s_i,s_j} that cannot be described exactly by Eq. (1).

2. Analysis of the model

Let us assume that a set of stimulus intensities $\mathfrak{S} = \{s_i; i = 1 \ldots n\}$ and a set of pairs $\mathfrak{P} = \{(s_i, s_j); s_i, s_j \in \mathfrak{S}\}$ define the measurement scheme. Furthermore, a set of model parameters $\vec{x} = \{R_i, \sigma_i; i = 1 \ldots n\} \in \mathbb{R}^{2n}$ defines a point in the parameter space and a set of performances $\vec{P} = \{P_{(s_i,s_j)}; (s_i, s_j) \in \mathfrak{P}\}$ defines the point in a measurement (performance) space. Thus, a set of equations

$$\mathfrak{E} = \left\{ P_{s_i,s_j} = \Phi\left(\frac{R_{s_j} - R_{s_i}}{\sqrt{\sigma_{s_i}^2 + \sigma_{s_j}^2}} \right); \{s_i, s_j\} \in \mathfrak{P} \right\} \tag{4}$$

defines the surface of possible performances and the mapping of points in the parameter space to the surface in the measurement space: $\mathfrak{E} : \vec{x} \mapsto \vec{P}$. The mapping is not reversible, namely, two points $\vec{x}$ and $\vec{x}'$ satisfying the set of Eqs. (2) or (3) are mapped to the same point $\vec{P}$.

Let us assume that the performance of the subject results from a ''true'' model with parameters $\vec{x}_t$, corresponding to the idealized performances $\vec{P}(\vec{x}_t)$. The model $\vec{x}$, estimated from the experimental data, will necessary correspond to different performances $\vec{P}(\vec{x})$. We therefore define a family of models with performances that are separated from the true one by an Euclidean distance ε:

$$\mathfrak{F}_\varepsilon = \left\{ \vec{x} : \sum_{(i,j)\in\mathfrak{P}} [P_{i,j}(\vec{x}) - P_{i,j}(\vec{x}_t)]^2 < \varepsilon^2 \right\}.$$

The distance element ds^2 at the point P on the surface $\mathfrak{E}$ can be expressed in terms of parameters using a metric tensor:

$$ds^2 = \sum_{(i,j)\in\mathfrak{P}} (dP_{i,j})^2 = \sum_{\mu,\nu=1}^{2n} g_{\mu\nu}\, dx_\mu\, dx_\nu, \tag{5}$$

$$g_{\mu\nu} = \sum_{(i,j)\in\mathfrak{P}} \frac{\partial P_{(i,j)}}{\partial x_\mu} \frac{\partial P_{(i,j)}}{\partial x_\nu}. \tag{6}$$

Using Eq. (4) the metric tensor can be expressed as follows:

$$g_{\mu\nu} = \sum_{(i,j)\in\mathfrak{P}} \left(\frac{d\Phi(Z_{(i,j)})}{dZ_{(i,j)}} \right)^2 \frac{\partial Z_{(i,j)}}{\partial x_\mu} \frac{\partial Z_{(i,j)}}{\partial x_\nu}, \tag{7}$$

where

$$Z_{(i,j)} = \frac{R_j - R_i}{\sqrt{\sigma_i^2 + \sigma_j^2}}. \tag{8}$$

The singularities in the metric tensor $g_{\mu\nu}$ mean that $ds^2 = 0$ along the zero eigenvectors and thus $\mathfrak{F}_\varepsilon$ will be much large than in non-singular case. Consequently, a family of models barely distinguishable from each other should be expected when the true model approaches a singular one, and there is no reasonable estimator that can dissociate these models.

The conditions for the metric tensor singularities are represented by the following equation (derived in Appendix A):

$$(\delta R_j - \delta R_i) - \frac{R_j - R_i}{\sigma_i^2 + \sigma_j^2} (\sigma_i \delta\sigma_i + \sigma_j \delta\sigma_j) = 0, \tag{9}$$

where δR and $\delta\sigma$ stand for small deviations of the parameters from R and σ correspondingly.

The metric tensor has two zero eigenvalues in the general case. The eigenvectors corresponding to these eigenvalues represent transformations that do not change the measured performances (the true continuous symmetry of the model, Eq. (2)): eigenvectors $\delta x_i = \{\delta R_i = 1, \delta\sigma_i = 0\}$ and $\delta x_i = \{\delta R_i = R_i, \delta\sigma_i = \sigma_i\}$ reflect the shift of mean internal responses and scaling of all parameters, correspondingly. Surprisingly, there is a subspace of internal parameters (R, σ), where other singularities appear.

Appendix B shows the derivation of all singularities of the metric tensor. There are three families of singularities except those defined by the model symmetry (presented in Table 1). Each family is parameterized by one, two, or three parameters. For each particular singular model $\vec{x}_0$ there is a family of models $\mathfrak{F}_\varepsilon(\vec{x}_0)$ differing slightly in performance but spanning a large range of parameters. Here, we can define a family of singular models as the family of models where at least one model is singular. It is straightforward to see that a family of singular models spans a larger space of parameters compared to families of non-singular models, for the same value of distance ε.

In order to illustrate the practical implication of the singularity, we analyze the properties of a family of models with performances close to the constant noise model ($\sigma_i = \sigma$, $\forall i$). Normally, the mean internal response is a

Table 1
Conditions for singularities of the metric tensor (Eq. (7))

σ	δR	$\delta\sigma$
any	$aR+b$	$a\sigma$
d	aR^2+bR+c	$d(2aR+b)$
$\sqrt{aR+b}$	$\frac{1}{aR+b}+dR+f$	$-a(aR+b)^{-\frac{3}{2}}+d\sqrt{aR+b}$
$\sqrt[4]{a(R+c)^2+b}$	$\sqrt{a(R+c)^2+b}+dR+f$	$\frac{a(R+c)}{\sqrt[4]{a(R+c)^2+b}}+d\sqrt[4]{a(R+c)^2+b}$

The first column represents the dependency of σ on R in each of the 4 conditions, and the two other columns represent the eigenvector components for singular eigenvalues. Here a, b, c, d, f are constants parameterizing the corresponding family of models.

monotonically increasing function of the stimulus intensity. Thus, in order to eliminate the symmetry of Eq. (1), we can set the minimal and maximal mean internal responses to zero and one, respectively. In this way we define a unique relationship between model parameters $\vec{x}$ and probabilities $\vec{P}$, except for the case of linear dependency of R and σ. Nevertheless, the transformation of the parameters along the additional singular eigenvector defines a one-parametric family of the models with $\vec{P}'(\gamma)$ approaching $\vec{P}$ (see details in Appendix C):

$$R'_i = \frac{(1+\gamma R_i)R_i}{1+\gamma},$$
$$\sigma'_i = \frac{(1+2\gamma R_i)\sigma}{1+\gamma}. \tag{10}$$

Here σ represents the noise in the constant noise model and γ is an arbitrary parameter (formally $\gamma \in [-\frac{1}{2}, +\infty)$). When γ deviates from zero, the distance between P and P' increases, and $\gamma = 0$ defines the constant noise model. The significance of singularity of the constant noise model is that the distance between P and P' grows slower than quadratically with γ, and thus the size of $\mathfrak{F}_\varepsilon$ shrinks much slower comparing to a non-singular case. Eqs. (10) parametrically define a relationship between R' and σ', which is illustrated in Fig. 2. This family of solutions can be explicitly expressed as

$$\sigma'_i = \frac{\sqrt{4\gamma(1+\gamma)R'_i+1}}{1+\gamma}\sigma. \tag{11}$$

Clearly, the resulting dependency defines a singular model (Table 1, third line). This leads to a dense cloud of singularities near the constant noise model.

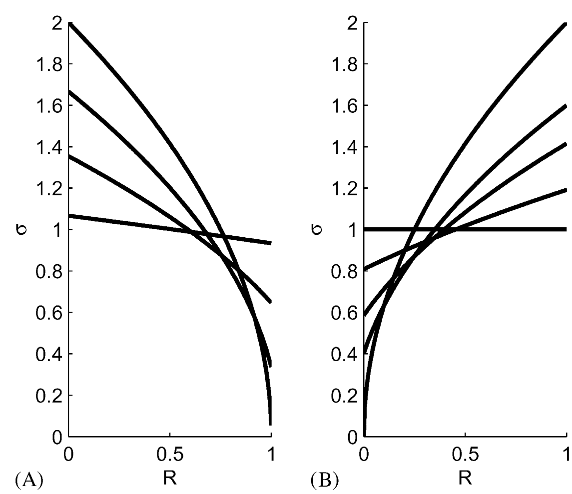

Fig. 2. Examples of the relationship between noise amplitudes and mean internal responses under conditions where the performances are close to the constant noise model. Different curves represent different values of the parameter γ. Curves with $\gamma<0$ (A) and $\gamma \geqslant 0$ (B) are shown.

3. Monte-Carlo simulations

To illustrate our theoretical findings, we performed Monte-Carlo simulations of the 2AFC experiment. Based on the simulated performances, we estimated the parameters of the model. In order to check the stability of the solution, the simulation-estimation procedure was repeated several times starting from the same initial conditions. For a singular case we expect much greater variability as compared with the non-singular case.

During the simulations, the mean internal response and the noise amplitude were fixed for each stimulus intensity (true model). Two random numbers (internal responses) were drawn from the normal distribution, with the mean and standard deviation being the mean internal response and the noise amplitude for the corresponding stimulus, during the simulation of each trial. The trial was considered as correct when the internal response for the stimulus with the higher intensity was greater than the internal response for other stimulus in the pair. Then, based on the trial responses, we computed the performances for each pair of stimuli as the percentage of correct discriminations. The least-squares estimator was used to reconstruct the parameters of the model. Finally, the parameters in all cases were normalized so that the lowest and highest mean internal responses were zero and one, respectively.

Fig. 3 depicts the estimated internal parameters obtained from the simulated performances. A large spread of model parameters was observed when the performances were simulated using the constant noise model for fifty different

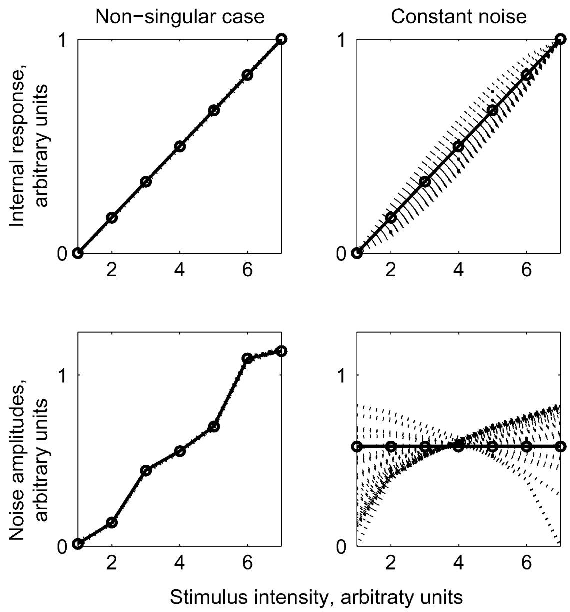

Fig. 3. Reconstruction of the mean internal response and noise amplitude in the Monte-Carlo simulations. The mean internal response and noise amplitudes reconstructed using the performances obtained in the Monte-Carlo simulations (see details in the text) are presented in the first and the second rows respectively. An estimation for fifty simulations is represented by the dotted lines, and the "true" model is represented by solid lines. Non-singular and constant noise cases are shown in the first and second columns, respectively.

simulated experiments with the same underlying model (a singular model, see Table 1, second row), and almost no spread with a non-singular model. The parameters in both cases were estimated based on the modeling of 40 000 trials for each pair of stimuli (which defines ε). All possible pairs were used in the simulation. The range of obtained values of P were comparable in both models (data not shown).

4. Discussion

Analytical calculations show the existence of three possible singularities in the estimation of internal model parameters from 2AFC data, in addition to those resulting from symmetry (Eqs. (2) and (3)). These singularities lead to difficulties in estimating the model parameters from the experimental data, since large differences in the parameters near a singularity produce small differences in the performance. One of the signs for the presence of singularity is the large confidence intervals in the estimated parameters. The reason for the singularity originates from the model, where the difference of two normal random variables is used. Thus, all methods employing such an approach (e.g. difference judgment) can potentially experience a singularity problem.

The present results show that data from 2AFC experiments should be treated with caution. In general, the set of the models $\mathfrak{F}_\varepsilon$ describing the data decreases with the length of the experiment. Nevertheless, the size of such set decreases much slower when $\mathfrak{F}_\varepsilon$ includes a singular model. Consequently, for reasonably long experiments it is not possible to estimate the parameters reliably. Moreover, if there is a singularity of the metric tensor (7), then any kind of estimator and any non-singular distance definition introduced into the P space will lead to the same problem in estimating the parameters. On the other hand, for models where the metric tensor does not have singularities, except the model symmetry, any reasonable estimator can be used to recover the model parameters.

In order to avoid singularities, the model should be modified. One way to do this, is to introduce some assumptions about internal responses and/or their variability, which remove singularity. Then, fit a new model using the same data. This is a good strategy, when someone looks for a model that describes the data, not necessarily a unique one. On the other hand, this is not always sufficient. For example, there is a strong debate whether the variance of internal responses depends on contrast or not (see Introduction). Any a priori assumption about the noise behavior eliminates the question, and allows to find a unique model. However, this assumption may not correspond to a "true" model. On the other hand, it seems to be possible to avoid singularities by using a different experimental scheme. For example, external noise can be used to move the system away from the singularity. In practice, external noise can be introduced into the experiment as a trial-by-trial variation of the stimulus intensity. Thus, the distribution of the internal responses will include variations due to the internal noise and the transduced external noise. One problem here is that, due to transducer nonlinearity, the contribution of the external noise to the internal distribution is not necessarily normally distributed. This problem can be minimized by using external noise with amplitudes small enough to allow a linear approximation around the mean. It is not clear, however, what magnitude of external noise is required to move the system away from singularity.

Another method that avoids singularities is the Thurstonian method of scaling on successive intervals (McNicol, 2005; Katkov, Tsodyks, & Sagi, 2006b). In this method, observers rate stimuli of different intensities using a subjective scale (e.g., 1 to 5 with 1 being the weakest stimulus and 5 the strongest). The model here assumes that each stimulus evokes an internal response and that the brain establishes a number of criteria (category boundaries). A particular scale value (category) is assumed to be reported when the internal response evoked by the stimulus is between the boundaries defined for that category. Thus, the probability of the reported class being greater than j can be represented in the following form:

$$P_{s_i,j} = \Phi\left(\frac{R_{s_i} - k_j}{\sqrt{\sigma^2_{s_i} + \sigma^2_{k_j}}}\right), \tag{12}$$

where s_i is a presented stimulus, k_j is a mean upper boundary for the j class, R_{s_i} is a mean internal response for the presented stimulus, σ_{s_i} is a standard deviation of the internal response and σ_{k_j} is a standard deviation of the boundary j. Formally, Eq. (12) has the same structure as Eq. (1), but in practice we do not expect the same singularities to emerge, since σ_s and σ_k have different origins. In fact, if σ_k is assumed to be independent of k, there will be no singularities in the solution of Eq. (1). Instead, an additional symmetry will appear. Such an assumption implies that all decision boundaries have equal variances.

Acknowledgments

The authors of this paper thank Dmitry Kerner and Dmitry Bibichkov for their help in the analytical calculations. This work was supported by the Israel Science Foundation (Grant #1065/03), and by the United States-Israel Binational Science Foundation. M.T. is partially supported by Irving B. Harris foundation.

Appendix A. Condition for singularities

We start from the metric tensor

$$g_{\mu\nu} = \sum_{(i,j)\in\mathfrak{P}} \left(\frac{d\Phi(Z_{(i,j)})}{dZ_{(i,j)}}\right)^2 \frac{\partial Z_{(i,j)}}{\partial x_\mu}\frac{\partial Z_{(i,j)}}{\partial x_\nu}. \tag{A.1}$$

We can express it in terms of the parameters of the model, R's and σ's, for which we must first compute the derivatives of the $Z_{(i,j)}$ values:

$$\frac{\partial Z_{(i,j)}}{\partial R_k} = \frac{\delta_{j,k}-\delta_{i,k}}{\sqrt{\sigma_i^2+\sigma_j^2}},$$
$$\frac{\partial Z_{(i,j)}}{\partial \sigma_k} = -(R_j-R_i)\frac{\sigma_i\delta_{i,k}+\sigma_j\delta_{j,k}}{(\sigma_i^2+\sigma_j^2)^{3/2}}, \tag{A.2}$$

where $\delta_{i,k}$ is a Kronecker delta symbol:

$$\delta_{i,k} = \begin{cases} 1, & i=k, \\ 0, & i\neq k. \end{cases}$$

Thus, the metric tensor has the following form:

$$g_{R_kR_m} = \sum_{(i,j)} \left(\frac{d\Phi(Z_{(i,j)})}{dZ_{(i,j)}}\right)^2 \frac{(\delta_{j,k}-\delta_{i,k})(\delta_{j,m}-\delta_{i,m})}{\sigma_i^2+\sigma_j^2},$$

$$g_{\sigma_kR_m} = -\sum_{(i,j)} \left(\frac{d\Phi(Z_{i,j})}{dZ_{i,j}}\right)^2 \frac{R_j-R_i}{(\sigma_i^2+\sigma_j^2)^2} \times(\sigma_i\delta_{i,k}+\sigma_j\delta_{j,k})(\delta_{j,m}-\delta_{i,m}),$$
$$g_{\sigma_k\sigma_m} = \sum_{(i,j)} \left(\frac{d\Phi(Z_{i,j})}{dZ_{i,j}}\right)^2 \frac{(R_j-R_i)^2}{(\sigma_i^2+\sigma_j^2)^3} \times(\sigma_i\delta_{i,k}+\sigma_j\delta_{j,k})(\sigma_i\delta_{i,m}+\sigma_j\delta_{j,m}). \tag{A.3}$$

Since we are looking for the singularities of the metric tensor, it is sufficient to find the solutions for the following system of equations:

$$\sum_\mu g_{\mu\nu}\delta x_\mu = 0. \tag{A.4}$$

Substituting Eqs. (A.3) into Eqs. (A.4) leads to

$$0 = \sum_k\sum_{(i,j)} \left(\frac{d\Phi(Z_{i,j})}{dZ_{i,j}}\right)^2 \frac{(\delta_{j,k}-\delta_{i,k})(\delta_{j,m}-\delta_{i,m})}{\sigma_i^2+\sigma_j^2}\delta R_k - \sum_k\sum_{(i,j)} \left(\frac{d\Phi(Z_{i,j})}{dZ_{i,j}}\right)^2 \frac{R_j-R_i}{(\sigma_i^2+\sigma_j^2)^2} \times(\sigma_i\delta_{i,k}+\sigma_j\delta_{j,k})(\delta_{j,m}-\delta_{i,m})\delta\sigma_k,$$

$$0 = -\sum_k\sum_{(i,j)} \left(\frac{d\Phi(Z_{i,j})}{dZ_{i,j}}\right)^2 \frac{R_j-R_i}{(\sigma_i^2+\sigma_j^2)^2} \times(\sigma_i\delta_{i,m}+\sigma_j\delta_{j,m})(\delta_{j,k}-\delta_{i,k})\delta R_k + \sum_k\sum_{(i,j)} \left(\frac{d\Phi(Z_{i,j})}{dZ_{i,j}}\right)^2 \frac{(R_j-R_i)^2}{(\sigma_i^2+\sigma_j^2)^3} \times(\sigma_i\delta_{i,k}+\sigma_j\delta_{j,k})(\sigma_i\delta_{i,m}+\sigma_j\delta_{j,m})\delta\sigma_k. \tag{A.5}$$

Taking the sum over k, we obtain

$$0 = \sum_{(i,j)} \left(\frac{d\Phi(Z_{i,j})}{dZ_{i,j}}\right)^2 \frac{(\delta_{j,m}-\delta_{i,m})}{\sigma_i^2+\sigma_j^2}(\delta R_j-\delta R_i) - \sum_{(i,j)} \left(\frac{d\Phi(Z_{i,j})}{dZ_{i,j}}\right)^2 \frac{R_j-R_i}{(\sigma_i^2+\sigma_j^2)^2} \times(\delta_{j,m}-\delta_{i,m})(\sigma_i\delta\sigma_i+\sigma_j\delta\sigma_j),$$

$$0 = \sum_{(i,j)} \left(\frac{d\Phi(Z_{i,j})}{dZ_{i,j}}\right)^2 \frac{R_j-R_i}{(\sigma_i^2+\sigma_j^2)^2}(\sigma_i\delta_{i,m}+\sigma_j\delta_{j,m}) \times(\delta R_j-\delta R_i) - \sum_{(i,j)} \left(\frac{d\Phi(Z_{i,j})}{dZ_{i,j}}\right)^2 \frac{(R_j-R_i)^2}{(\sigma_i^2+\sigma_j^2)^3} \times(\sigma_i\delta_{i,m}+\sigma_j\delta_{j,m})(\sigma_i\delta\sigma_i+\sigma_j\delta\sigma_j). \tag{A.6}$$

Combining the terms, we obtain:

$$0 = \sum_{(i,j)} \left(\frac{d\Phi(Z_{i,j})}{dZ_{i,j}}\right)^2 \frac{(\delta_{j,m}-\delta_{i,m})}{\sigma_i^2+\sigma_j^2} \times\left[(\delta R_j-\delta R_i) - \frac{R_j-R_i}{\sigma_i^2+\sigma_j^2}(\sigma_i\delta\sigma_i+\sigma_j\delta\sigma_j)\right],$$

$$0 = \sum_{(i,j)} \left(\frac{d\Phi(Z_{i,j})}{dZ_{i,j}}\right)^2 \frac{R_j-R_i}{(\sigma_i^2+\sigma_j^2)^2}(\sigma_i\delta_{i,m}+\sigma_j\delta_{j,m}) \times\left[(\delta R_j-\delta R_i) - \frac{R_j-R_i}{\sigma_i^2+\sigma_j^2}(\sigma_i\delta\sigma_i+\sigma_j\delta\sigma_j)\right]. \tag{A.7}$$

Thus, the metric tensor has a singularity when the expression in the square brackets equals zero. If at least one of the brackets is not zero, but the global sum is zero due to accidental cancellation of terms, then removing the pair which has a non-zero expression in the bracket, eliminates the singularity. Thus, the condition for the singularity, that does not depend on the particular choice of the pairs used in the experiment is

$$(\delta R_j - \delta R_i) - \frac{R_j - R_i}{\sigma_i^2 + \sigma_j^2}(\sigma_i \delta\sigma_i + \sigma_j \delta\sigma_j) = 0 \tag{A.8}$$

for all stimulus pairs (i,j). Eq. (A.8) is an equation for the eigenvector $(\delta R_i, \delta\sigma_i)$ for given model parameters (R_i, σ_i). We are looking for the condition for (R_i, σ_i) that guarantees that Eq. (A.8) has a non-trivial solution.

Appendix B. Derivation of singularities

Eq. (A.8) is defined for a set of stimuli, but, since we are looking for the singularity conditions that do not depend on the particular choice of the stimulus intensities, we extend this equation to the continuous limit:

$$\rho(y) - \rho(x) - \frac{y - x}{\sigma(x)^2 + \sigma(y)^2}(\sigma(x)\xi(x) + \sigma(y)\xi(y)) = 0. \tag{B.1}$$

Since $R_i = R(c_i)$ and $R(c)$ is a monotonic function of contrast c, we can substitute variables, so that $R(c) = x$. This redefines the function $\sigma(R(c)) = \sigma(x)$, which is now a function of x. Thus, $\rho(c_i) = \delta R_i$ and $\xi(c_i) = \delta\sigma_i$; c_i represents an intensity of the stimulus i; $\sigma(x) > 0, \forall x$, $\rho(x) \in \mathbb{R}$. Solving this functional equation on ρ and ξ for arbitrary $\sigma(x)$, we will obtain all possible singularities together with the conditions regarding the forms of σ where these singularities appear.

The left part of Eq. (B.1) equals zero when $x = y$. Thus, we are looking for cases when $y \neq x$. We divide Eq. (B.1) by $(y - x)$, and obtain

$$\frac{\rho(y) - \rho(x)}{y - x} - \frac{\sigma(x)\xi(x) + \sigma(y)\xi(y)}{\sigma(x)^2 + \sigma(y)^2} = 0.$$

Then we take a limit of $y \to x$, and obtain

$$\rho'(x) = \frac{\xi(x)}{\sigma(x)}.$$

Thus,

$$\xi(x) = \sigma(x)\rho'(x). \tag{B.2}$$

Substituting Eq. (B.2) into Eq. (B.1) leads to

$$\rho(y) - \rho(x) - \frac{y - x}{\sigma(x)^2 + \sigma(y)^2}(\sigma(x)^2\rho'(x) + \sigma(y)^2\rho'(y)) = 0.$$

Multiplying it by $\sigma(x)^2 + \sigma(y)^2$ gives

$$(\rho(y) - \rho(x))(\sigma(x)^2 + \sigma(y)^2) - (y - x)(\sigma(x)^2\rho'(x) + \sigma(y)^2\rho'(y)) = 0.$$

Introducing a new variable $s(x) = \sigma(x)^2 > 0$, we have

$$(\rho(y) - \rho(x))(s(x) + s(y)) - (y - x)(s(x)\rho'(x) + s(y)\rho'(y)) = 0.$$

Then, we take a derivative with respect to x, and obtain

$$-\rho'(x)(s(x) + s(y)) + (\rho(y) - \rho(x))s'(x) + (s(x)\rho'(x) + s(y)\rho'(y)) - (y - x)(s'(x)\rho'(x) + s(x)\rho''(x)) = 0,$$

collecting terms, we obtain

$$(\rho'(y) - \rho'(x))s(y) + (\rho(y) - \rho(x) - \rho'(x)(y - x))s'(x) - (y - x)s(x)\rho''(x) = 0.$$

We take a derivative with respect to x a second time, and obtain

$$-\rho''(x)s(y) - 2\rho''(x)(y - x)s'(x) + (\rho(y) - \rho(x) - \rho'(x) \times (y - x))s''(x) + s(x)\rho''(x) - (y - x)s(x)\rho'''(x) = 0.$$

Collecting the terms together and changing a global sign, we obtain

$$\rho''(x)[s(y) - s(x) + 2(y - x)s'(x)] - (\rho(y) - \rho(x) - \rho'(x) \times (y - x))s''(x) + (y - x)s(x)\rho'''(x) = 0. \tag{B.3}$$

Dividing Eq. (B.3) by $(y - x)$ yields

$$s(x)\rho'''(x) + \rho''(x)\left[\frac{s(y) - s(x)}{y - x} + 2s'(x)\right] - s''(x)\left[\frac{\rho(y) - \rho(x)}{y - x} - \rho'(x)\right] = 0.$$

Taking the limit $y \to x$, we obtain

$$3\rho''(x)s'(x) + s(x)\rho'''(x) = \frac{[s(x)^3\rho''(x)]'}{s(x)^2} = 0. \tag{B.4}$$

Taking a y derivative of Eq. (B.3) yields

$$\rho''(x)[s'(y) + 2s'(x)] - (\rho'(y) - \rho'(x))s''(x) + s(x)\rho'''(x) = 0.$$

Substituting Eq. (B.4), we obtain

$$\rho''(x)[s'(y) - s'(x)] - (\rho'(y) - \rho'(x))s''(x) = 0$$

and taking the second derivative, we obtain

$$\rho''(y)s''(x) - \rho''(x)s''(y) = 0.$$

Finally,

$$\frac{\rho''(y)}{s''(y)} = \frac{\rho''(x)}{s''(x)} = \text{const}.$$

When $s''(x)$ exists and $s''(x) \neq 0$, we have

$$\rho(x) = \alpha s(x) + \beta x + \gamma.$$

On the other hand, Eq. (B.4) puts the constraint on $s(x)$:

$$\rho''(x) = \frac{\text{const}}{s(x)^3},$$

$$\frac{\rho''(x)}{s''(x)} = \frac{\text{const}}{s(x)^3 s''(x)} = \text{const}.$$

Thus, $s(x)^3 s''(x) = \text{const}$. Starting from equation

$$s(x)^3 s''(x) = c_1. \tag{B.5}$$

We multiply it by $2\frac{s'(x)}{s(x)^3}$ yielding

$$2s'(x)s''(x) = [(s'(x))^2]' = 2c_1 \frac{s'(x)}{s(x)^3}.$$

Taking an integral and redefining c_1 we obtain

$$(s'(x))^2 = \frac{c_1}{s(x)^2} + c_2.$$

Multiplying it by $s(x)^2$, we obtain

$$(s(x)s'(x))^2 = \left(\frac{[s(x)^2]'}{2}\right)^2 = c_1 + c_2 s(x)^2$$

and introducing a new variable $\zeta(x) = s(x)^2$, we obtain

$$(\zeta'(x))^2 = c_1\zeta(x) + c_2$$

or

$$\zeta'(x) = \sqrt{c_1\zeta(x) + c_2}. \tag{B.6}$$

Since $\zeta(x)$ is a positive real function, this equation applies a constraint to the parameters c_1 and c_2:

$$\frac{c_2}{c_1} > -\min_x \zeta(x).$$

The solution of Eq. (B.6) is

$$\zeta(x) = \frac{c_1}{4}(x + c_3)^2 - \frac{c_2}{c_1}.$$

Thus,

$$\zeta(x) = s(x)^2 = \sigma(x)^4 = \frac{c_1}{4}(x + c_3)^2 - \frac{c_2}{c_1}$$

and

$$\sigma(x) = \sqrt[4]{\frac{c_1}{4}(x + c_3)^2 - \frac{c_2}{c_1}}.$$

The expression under the root should be positive. If no constraint on x is applied then $c_1 > 0$ and $c_2 < 0$.

If $s''(x) = 0$, then either $s(x) = \text{const}$, or $s(x) = ax + b$. If $s(x) = \text{const}$, then Eq. (B.1) can be written as

$$\rho(y) - \rho(x) - \frac{(y - x)(\xi(x) + \xi(y))}{2\sigma} = 0.$$

Substituting Eq. (B.2) yields

$$\rho(y) - \rho(x) - (y - x)\frac{\rho'(x) + \rho'(y)}{2} = 0.$$

Taking a derivative with respect to y, we obtain

$$\rho'(y) - \rho'(x) - (y - x)\rho''(y) = 0.$$

Taking a derivative with respect to x, we obtain

$$\rho''(x) = \rho''(y) = \text{const}.$$

Thus,

$$\rho(x) = ax^2 + bx + c, \quad \xi(x) = \sigma(2ax + b).$$

And in the last case, when $s(x) = ax + b$, Eq. (B.1), after substituting Eq. (B.2), becomes

$$\rho(y) - \rho(x) - \frac{y - x}{a(x + y) + 2b}((ax + b)\rho'(x) + (ay + b)\rho'(y)) = 0.$$

Multiplying it by $a(x + y) + 2b$ gives

$$(\rho(y) - \rho(x))(a(x + y) + 2b) - (y - x)((ax + b)\rho'(x) + (ay + b)\rho'(y)) = 0.$$

Taking the derivative with respect to y gives

$$\rho'(y)(ax + b) + a(\rho(y) - \rho(x)) - (ax + b)\rho'(x) - (y - x)(a\rho'(y) + (ay + b)\rho''(y)) = 0.$$

Taking a derivative with respect to x gives

$$a\rho'(y) - a\rho'(x) - a\rho'(x) - (ax + b)\rho''(x) + a\rho'(y) + (ay + b)\rho''(y) = 0$$

and combining the terms together, yields

$$2a\rho'(y) + (ay + b)\rho''(y) = 2a\rho'(x) + (ax + b)\rho''(x) = \text{const}.$$

Thus,

$$2a(ax + b)\rho'(x) + (ax + b)^2\rho''(x) = c(ax + b),$$

where c is some constant that we will redefine in the following calculations as needed. Combining the terms in the left part we obtain

$$[(ax + b)^2\rho'(x)]' = c(ax + b).$$

Thus,

$$(ax + b)^2\rho'(x) = c(ax + b)^2 + d,$$

where d is another constant, and

$$\rho'(x) = c + \frac{d}{(ax + b)^2}.$$

Finally,

$$\rho(x) = cx + f + \frac{d}{ax + b}.$$

Here a and b are parameters of the singularity, and c, d and f are some constants.

Finally, there are four different types of singularities expressed in terms of R, which are presented in Table 1.

Appendix C. A family of models for the constant noise singularity

We are interested in a family of solutions $\mathfrak{F}_\varepsilon, \varepsilon \to 0$ that is generated by the constant noise model (R, σ). In order to find it we perform transformations to the constant noise solutions along three singular eigenvectors. The following transformations are used:

"Shift"	"Scale"	"Nonlinear"
$R_i \to R_i + \alpha$ $\sigma_i \to \sigma_i$	$R_i \to \beta R_i$ $\sigma_i \to \beta\sigma_i$	$R_i \to R_i\ (1+\gamma R_i)$ $\sigma_i \to \sigma_i\ (1+2\gamma R_i)$

Here, α, β, and γ are certain parameters. By the nature of the transformation, $\beta > 0$, γ is a small parameter, and α is a real number. We can normalize the transducer function by putting three constraints: (1) $R'_i = 0$, when $R_i = 0$; (2) $R'_i = 1$, when $R_i = 1$; (3) R', like R, is a monotonically increasing function. In this way the mapping will be unique. Three transformations can now be applied in any order and despite the presence of the nonlinear transformation they are either equivalent or do not satisfy the normalization constraints. Next, we present an analysis of a particular transformation. The analysis of the remaining five transformation sequences is identical and does not add any information, and thus, is not presented here.

Here, we analyze the family of solutions obtained by applying a sequence of transformations to the constant noise model. The sequence is as follows: "shift", "nonlinear" and "scale". Thus, we can write the following sequence of R's and σ's:

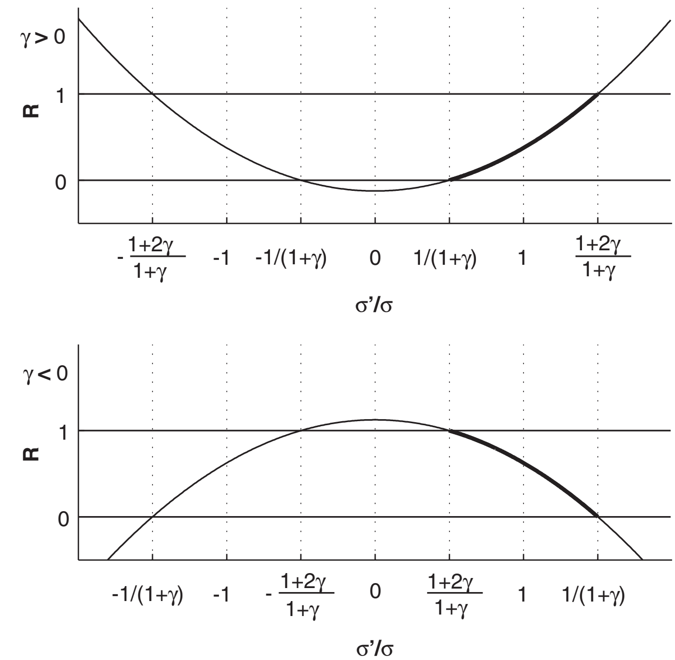

Fig. 4. The relationship between R and σ defined by Eq. (C.9). The solid line represents the resulting dependency of σ on R. All solutions from the family cross the original constant noise model. When γ becomes too negative, the curve does not reach line $R = 1$, and there is no mapping between the constant noise model and the transformed one. Therefore, these values of γ are invalid.

	Operation	R	σ
1	"Shift"	$R_i^{(1)} = R_i + \alpha$	$\sigma_i^{(1)} = \sigma$
2	"Nonlinear"	$R_i^{(2)} = (R_i + \alpha)(1 + \gamma(R_i + \alpha))$	$\sigma_i^{(2)} = \sigma(1 + 2\gamma(R_i + \alpha))$
3	"Scale"	$R_i^{(3)} = \beta(R_i + \alpha)(1 + \gamma(R_i + \alpha))$	$\sigma_i^{(3)} = \beta\sigma(1 + 2\gamma(R_i + \alpha))$

After the transformation we apply the constraints:

$$0 = \alpha\beta(1 + \alpha\gamma), \tag{C.1}$$

$$1 = \beta(1 + \alpha)(1 + \gamma(1 + \alpha)). \tag{C.2}$$

Since $\beta > 0$, then there are two possible solutions for the coefficients: either $\alpha = 0$ or not. If $\alpha \neq 0$, then

$$1 + \alpha\gamma = 0 \quad \text{from (C.1)} \tag{C.3}$$

$$(1 + \alpha)\beta\gamma = 1 \quad \text{from (C.2) and (C.3)} \tag{C.4}$$

$$\beta\gamma - \beta = 1, \tag{C.5}$$

$$\beta = \frac{1}{\gamma - 1}. \tag{C.6}$$

So, for $\beta > 0$, we must have $\gamma > 1$, which is a large number, but even for that large number, a transformed R_i will not be a monotonic function. Thus it is an impossible transformation.

If $\alpha = 0$, then

$$\beta = \frac{1}{1 + \gamma}.$$

Substituting the values of the parameters into transformed vectors, we obtain:

$$R'_i = \frac{R_i\ (1 + \gamma R_i)}{1 + \gamma} \tag{C.7}$$

and

$$\sigma'_i = \frac{\sigma\ (1 + 2\gamma R_i)}{1 + \gamma}. \tag{C.8}$$

From Eq. (C.8) we can find an expression for R_i and then substitute it in Eq. (C.7). In this way, we will obtain a functional dependency of R on σ for a family of the solutions experimentally equivalent to the model, with all $\sigma_i = \sigma$.

$$R_i = \frac{1}{2\gamma}\left(\frac{(1+\gamma)\sigma'_i}{\sigma} - 1\right),$$
$$R'_i = \frac{1}{4\gamma(1+\gamma)}\left(\frac{\sigma_i^{2'}}{\sigma^2}(1+\gamma)^2 - 1\right). \tag{C.9}$$

Two possible dependencies for $\gamma > 0$ and $\gamma < 0$ are shown in Fig. 4. The part of the solutions that we are interested in lies between $R = 0$ and $R = 1$, and $\sigma > 0$ is relevant. Formally, $\gamma \in [-\frac{1}{2}, +\infty)$, but in practice is defined by an experimental error. For values $\gamma < -\frac{1}{2}$, σ' becomes negative for R approaching zero or one.

References

Foley, J. M., & Legge, G. E. (1981). Contrast detection and near threshold discrimination in human vision. *Vision Research*, *21*, 1041–1053.

Gorea, A., & Sagi, D. (2001). Disentangling signal from noise in visual contrast discrimination. *Nature Neuroscience*, *4*(11), 1146–1150.

Green, D. M., & Swets, J. A. (1966). *Signal detection theory and psychophysics*. New York: Wiley.

Iverson, G. J. (1987). Thurstonian psychophysics: Case III. *Journal of Mathematical Psychology*, *31*, 219–247.

Katkov, M., Tsodyks, M., & Sagi, D. (2006a). Singularities in the inverse modeling of 2AFC contrast discrimination data. *Vision Research*, 46, 259–266.

Katkov, M., Tsodyks, M., & Sagi, D. (2006b). Inverse modeling of human contrast response. *Vision Research*, submitted for publication.

Kontsevich, L. L., Chen, C. C., & Tyler, C. W. (2002). Separating the effects of response nonlinearity and internal noise psychophysically. *Vision Research*, *42*(14), 1771–1784.

Lu, Z. L., & Dosher, B. A. (1999). Characterizing human perceptual inefficiencies with equivalent internal noise. *Journal of the Optical Society of America A*, *16*, 764–778.

McNicol, D. (2005). *A primer of signal detection theory*. Mahwah: Lawrence Erlbaum Associates.

Thurstone, L. L. (1927). A law of comparative judgment. *Physiological Review*, *34*, 273–287.

Torgerson, W. S. (1958). *Theory and method of scaling*. New York: Wiley.